CHAPTER FIVE

Metal Ion-Based RNA Cleavage as a Structural Probe

Marcello Forconi* *and* Daniel Herschlag†

Contents

Abstract

It is well established that many metal ions accelerate the spontaneous degradation of RNA. This property has been exploited in several ways to garner information about RNA structure, especially in regards to the location of site-specifically bound metal ions, the presence of defined structural motifs, and the occurrence of conformational changes in structured RNAs. In this chapter, we review this information, briefly giving strengths and limitations for each of these approaches. Finally, we provide a general protocol to perform metal ion-mediated cleavage of RNA.

* Department of Biochemistry, Stanford University, Stanford, California, USA
† Departments of Biochemistry and Chemistry, Stanford University, Stanford, California, USA

Methods in Enzymology, Volume 468
ISSN 0076-6879, DOI: 10.1016/S0076-6879(09)68005-8

1. Introduction

RNA molecules fold in intricate three-dimensional structures that are crucial for their biological functions. Metal ions play key roles in this process. Diffusely bound metal ions (often referred to as ''the ion atmosphere'') neutralize the negative charge present on the phosphodiester backbone, allowing nucleic acids to adopt globular structure. More specifically bound metal ions help to bring distant residues together, and shape certain motifs allowing the nucleic acid to adopt a well-defined three-dimensional structure. In addition, site-specifically bound metal ions may be involved in catalysis by nucleic acid enzymes; in particular, several RNA enzymes (ribozymes) use strategically positioned Mg^{2+} ions to help catalysis (Fedor, 2002; Frederiksen *et al.*, 2009). A key part in understanding RNA structure and function is to identify the interactions made by the specifically bound metal ions with the RNA, and how these interactions change in response to different conditions and reaction steps.

Mg^{2+} and other metal ions can promote cleavage of nucleic acids when added in micro- to millimolar quantities to solution (Breslow and Huang, 1991; Dimroth *et al.*, 1950; Farkas, 1968; Huff *et al.*, 1964). In principle, this ability of metal ions to promote RNA cleavage has the potential to reveal regions of the RNA molecule in close proximity to metal ions. For example, this ability may reveal sites of the molecule exposed to ion-atmosphere metal ions, and thus lying on the outer part of the folded RNA molecule, or sites in proximity of tightly bound metal ions.

However, as described in this chapter, the cleavage pattern of RNA molecules in the presence of metal ions is affected by many factors, and it is often impossible to interpret this pattern in terms of a single structural parameter, such as proximity between metal ions and the RNA backbone. Nevertheless, comparison of cleavage patterns in different conditions, for example, upon binding of a substrate to ribozyme, can provide information about local changes, complementing and expanding structural information that can be obtained using other techniques.

2. Mechanisms of Metal Ion-Based Cleavage of Nucleic Acids

Metal ions are known to promote cleavage of nucleic acid in aqueous solution. Typically, simple phosphate esters or dinucleotides are used in model studies to determine the rate acceleration provided by metal ions (Mikkola *et al.*, 2001; Oivanen *et al.*, 1998). Lanthanide ions, such as Eu^{3+}, Tb^{3+}, and Yb^{3+}, are particularly efficient in catalyzing cleavage of simple

dinucleotides, with rate acceleration of 3–4 orders of magnitude over the uncatalyzed reaction (Breslow and Huang, 1991). Pb^{2+}, Zn^{2+}, and to some extent Mg^{2+} also display rate acceleration over the uncatalyzed reaction (Breslow and Huang, 1991).

In general, cations with a low pK_a of their hydrates (Table 5.1) cleave RNA better than cations with a high pK_a. This is consistent with the proposal (Brown *et al.*, 1985) that hydrated metal ions cleave RNA acting as Brönsted bases, abstracting a proton from the 2′-OH group of the ribose (Fig. 5.1). This base generates a 2′-O^- group that attacks the phosphorous atom, with departure of the 5′-hydroxyl group. This reaction is greatly facilitated by a particular geometry, referred to as ''in-line'' geometry,

Table 5.1 Properties of some multivalent cations

Ion	Ionic radius (Å)	Coordination number	First pK_a of $[M(H_2O)_x]$
Mg^{2+}	0.57–0.89	6	11.4
Ca^{2+}	0.99	8	12.6
Mn^{2+}	0.66–0.96	4,6,8	10.6
Zn^{2+}	0.60–0.90	4,6,8	8.2–9.8
Ni^{2+}	0.55–0.69	4,6	6.5–10.2
Fe^{2+}	0.63	4	6.0–6.7
Co^{2+}	0.72	6	7.6–9.9
Pb^{2+}	0.98–1.5	4,6,8,10,12	6.5–8.4
UO_2^{2+}	0.8 (U^{6+})	6,8	5.7
Eu^{3+}	0.95	9	4.8–8.5
Tb^{3+}	0.92	8–9	8.2
Yb^{3+}	0.86	6–9	

Values are from Dallas *et al.* (2004), Frederiksen *et al.* (2009), and references therein.

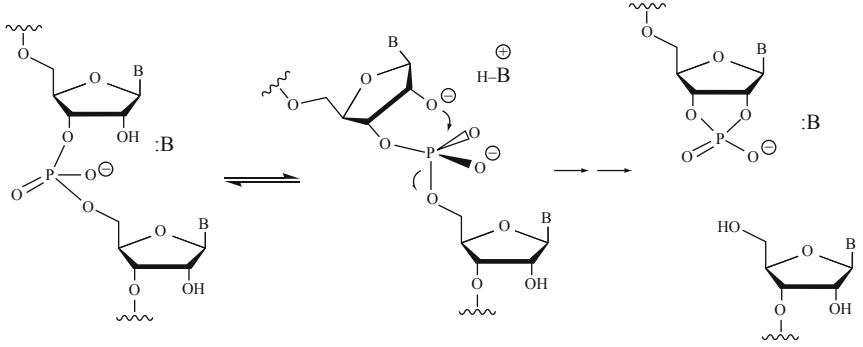

Figure 5.1 Possible mechanism of base-induced cleavage of RNA. Figure adapted from Kirsebom and Ciesiolka (2005).

whereby the attacking nucleophile and the leaving group are positioned about 180° from one another (Westheimer, 1968). Although the mechanism in which a metal ion facilitates abstraction of a proton from the 2′-OH group of the ribose is consistent with the experimental observations, it is not the only possibility (Arnone *et al.*, 1971; Butzow and Eichhorn, 1971). Indeed, alternative mechanisms of metal ion-mediated cleavage of RNA occur in natural RNA enzymes (ribozymes), as shown in Fig. 5.2 (Frederiksen *et al.*, 2009). In particular, metal ions can contribute to stabilization of the developing negative charge on the leaving group (Fig. 5.2A), on the nucleophile (Fig. 5.2B), and on the nonbridging phosphoryl oxygen atom (Fig. 5.2C). Further, they may coordinate both the nucleophile and the nonbridging phosphoryl oxygen (Fig. 5.2D), stabilizing the in-line geometry required for phosphoryl transfer reactions.

In addition, metal ions may impact catalysis through indirect effect. For example, they may constrain the RNA backbone so that the in-line attack of a distal 2′-hydroxyl is facilitated. Electrostatic stabilization of the transition state of the cleavage reaction through outer-sphere or long-range interactions is also possible, although not established.

Finally, it is important to point out that single-stranded regions in RNA are spontaneously cleaved by the mechanism in Fig. 5.1 ~100-fold more effectively than double-stranded regions, because single-stranded regions can sample the in-line conformation required for cleavage more often than double-stranded regions (Soukup and Breaker, 1999). According to this observation, metal ions are expected to generally be more effective in cleaving single-stranded regions of RNA (Hall *et al.*, 1996; Husken *et al.*, 1996; Kolasa *et al.*, 1993; Zagorowska *et al.*, 1998).

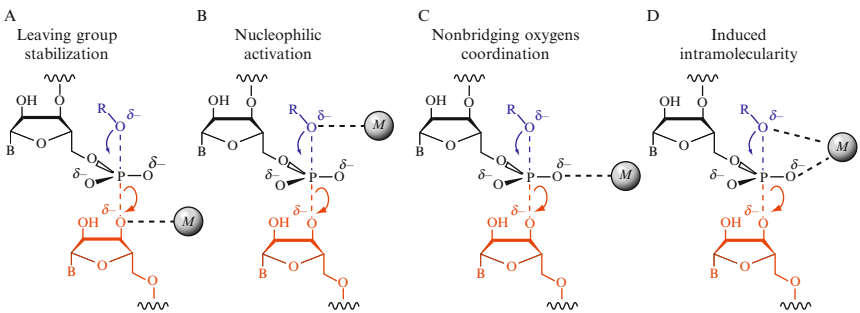

Figure 5.2 Additional strategies used by divalent metal ions to accelerate nucleophilic phosphotransesterification. (A) Lewis acid stabilization of the leaving group 3′-oxygen. (B) Activation of the incoming nucleophile. (C) Coordination of nonbridging oxygen atoms. (D) Induced intramolecularity, in which the external nucleophile and a nonbridging oxygen are coordinated by a metal ion. Figure adapted from Frederiksen *et al.* (2009).

3. Metal Ion-Based Cleavage of RNA as a Structural Probe

In this section, we briefly outline how metal ion-based cleavage of RNA has been used to garner structural information. We have used the excellent review by Kirsebom and Ciesiolka (2005) as a starting point for our considerations, and the reader is encouraged to read this original work. As outlined in that review, metal ion-mediated cleavage of RNA has been used in structural analysis of RNA and RNA complexes in two main ways: (i) to probe metal ion binding sites and (ii) to probe RNA structure and RNA–ligand interactions.

3.1. Probing metal ion binding sites

Metal ion-mediated cleavage of RNA to probe metal ion binding sites has been used in various RNAs, including tRNA (Ciesiolka *et al.*, 1989; Krzyzosiak *et al.*, 1988; Sampson *et al.*, 1987), group I (Rangan and Woodson, 2003; Streicher *et al.*, 1993, 1996) and group II (Sigel *et al.*, 2000) ribozymes, RNase P RNA (Brannvall *et al.*, 2001; Kaye *et al.*, 2002; Kazakov and Altman, 1991), the HDV ribozyme (Lafontaine *et al.*, 1999; Matysiak *et al.*, 1999; Rogers *et al.*, 1996), and the 16S and 23S subunits in the 70S ribosome (Dorner and Barta, 1999; Winter *et al.*, 1997). Because of their high affinity for RNA, lanthanide ions (especially Tb^{3+}) are commonly used in these experiments, although Pb^{2+}, Mn^{2+}, Fe^{2+}, and other metal ions (including Mg^{2+}) have also been used. The idea that underlies these experiments is that a strong metal ion-induced cleavage suggests the presence of a specific metal-ion binding site and that the residues involved in the coordination of the metal ion are close to the site of cleavage. This idea relies on several assumptions.

First, it implies that metal ions other than Mg^{2+} can displace Mg^{2+} from its high-affinity binding sites. This assumption is supported by the observation of relaxed-specificity of metal ion binding sites in two model RNAs, the P4–P6 domain of the *Tetrahymena* group I ribozyme (Travers *et al.*, 2007) and an engineered allosteric ribozyme (Zivarts *et al.*, 2005). However, it is not clear whether trivalent metal ions, such as Tb^{3+}, can effectively replace Mg^{2+} in its binding sites and in some cases the sites of bound metal ions are known to vary (e.g., Basu and Strobel, 1999; Jack *et al.*, 1977). Disappearance of the metal ion-induced cleavage when increasing quantities of Mg^{2+} are added is often taken as further support for this assumption. However, this interpretation is not unequivocal, as the disappearance of a band can also be due to indirect effects, such as changes in structure or simply replacement of the ion-atmosphere metal ions.

The second assumption is that the cleavage event can be ascribed to the abstraction of a proton from a 2′-OH group positioned near to the metal ion. Although this is reasonable, it is important to consider also the alternative mechanisms presented above, including the ones without direct involvement of the metal ion in the cleavage event. Further, it is possible that regions of the RNA only transiently sample the space near a metal ion, but nevertheless get cleaved more than other regions because of favorable geometry.

The third assumption is that the sites of cleavage are responsible for coordination of metal ions. However, there is no guarantee that just because a 2′-OH is nearby to a metal ion, it will act as a ligand for that metal ion or allow proton abstraction via a metal ion-coordinated hydroxide.

Finally, some metal ions may not be able to coordinate a water molecule, or coordinate it in the right place for the cleavage event, and rigid binding sites may be limited in cleavage efficiency. Secondary structure formation may complicate this analysis. As mentioned above, single-stranded regions are cleaved by metal ions more effectively than double-stranded regions (Hall *et al.*, 1996; Husken *et al.*, 1996; Kolasa *et al.*, 1993; Zagorowska *et al.*, 1998), and therefore metal ions bound to or near double-stranded regions may not cleave the RNA backbone efficiently. In addition, rigidity of metal ion binding sites may affect cleavage of metal ions located within the active sites of ribozymes. Because catalysis requires precise positioning of the catalytic residues, including metal ions, rigidity of active site metal ion binding sites may be used by ribozymes to contribute to precise positioning of the metal ion. However, metal ion-mediated cleavage of RNA may be more effective in regions more flexible, which presumably reside outside the active site. In this respect, it is interesting to note that the strongest sites of metal ion-induced cleavage for two ribozymes, the group I intron (Rangan and Woodson, 2003; Streicher *et al.*, 1993, 1996) and the RNase P RNA (Brannvall *et al.*, 2001; Kaye *et al.*, 2002; Kazakov and Altman, 1991), correspond to regions near metal ions located outside the active site, as shown by subsequent structural studies (Kazantsev *et al.*, 2009; Stahley and Strobel, 2007).

In summary, in the absence of other structural data, metal ion-induced cleavage of RNA may provide hints about the location of some metal ions, but it cannot establish the atoms involved in coordination of these metal ions or the importance of these metal ion in folding and catalysis. This technique can be used more powerfully to provide other structural information, as explained in Section 3.2.

3.2. Probing RNA structure and RNA–ligand interactions

Pb^{2+} and Tb^{3+} have been extensively used to probe RNA structure, usually employing higher quantities (millimolar) compared to experiments aimed at probing metal ion binding sites.

Pb^{2+}-mediated cleavage has been historically used with the assumption that more ''flexible'' regions (such as single-stranded regions) are cleaved better than more ''rigid'' regions (such as paired regions), as described above. Determining the cleavage pattern of an RNA in the presence of Pb^{2+} may reveal such regions. This approach is complementary to well-established approaches that use nucleases to detect such regions, has similar drawbacks, and presents additional complications due to the possibility that additional cleavage events may arise at high Pb^{2+} concentration from altered RNA conformations or from nonspecific Pb^{2+}-induced cleavage. Pb^{2+}-mediated cleavage has also been proposed as a technique to identify structural motifs in RNA molecules of unknown structure, based on the observation that the cleavage pattern of several structural motifs is identical independent of the rest of the RNA molecule (Ciesiolka *et al.*, 1998). These motifs are shown in Fig. 5.3.

Further, Pb^{2+}-mediated cleavage has been used in RNA–ligands complexes to identify regions of contacts between RNA and ligands (see Kirsebom and Ciesiolka, 2005, and references therein). This technique can match the information obtained with more established footprinting

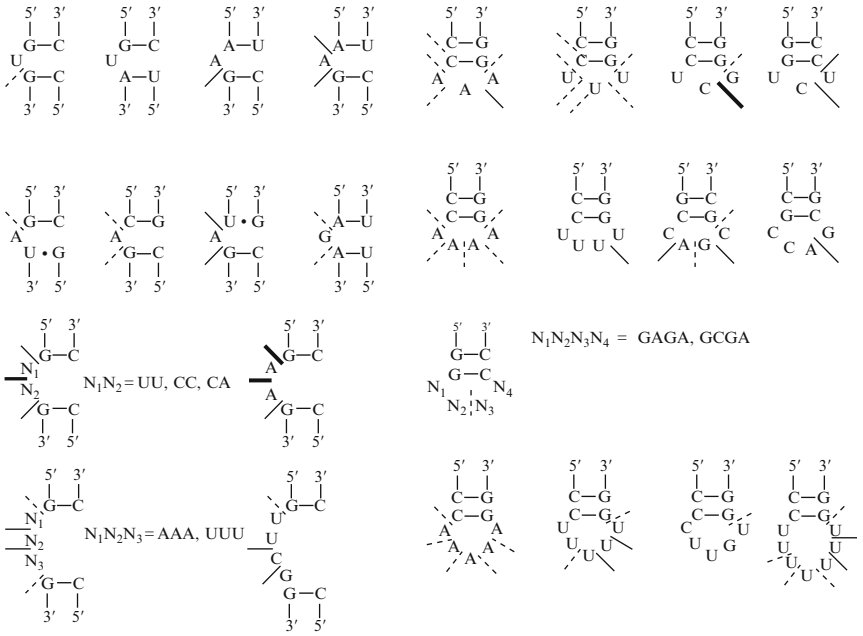

Figure 5.3 Cleavages induced by Pb^{2+} in RNA bulge regions (left panel) and terminal hairpin loops (right panel). Cleavage sites and their relative intensities are marked by lines—dotted lines: weak cleavages; normal lines: strong cleavages; thick lines: very strong cleavages. Figure adapted from Ciesiolka *et al.* (1998).

techniques, such as hydroxyl-radical footprinting. Because of the ambiguity of the metal ion-induced cleavage in comparison to hydroxyl-radical-mediated cleavage, the use of Pb^{2+} (or other metal ions) to probe RNA–ligands interactions seems to be at most complementary to other techniques.

Tb^{3+}-mediated cleavage of RNA has been introduced more recently as a technique to probe dynamics in RNA. In particular, structural changes in tRNA upon binding of HIV neurocapsid protein (Hargittai *et al.*, 2001) and in the *trans*-acting version of the HDV ribozyme upon binding of an oligonucleotide product or substrate (Jeong *et al.*, 2003) have been detected using this technique. In case of the HDV ribozyme, the differences in cleavage pattern with and without bound oligonucleotides were consistent with a structural change proposed on the basis of other techniques, such as fluorescence resonance energy transfer (Pereira *et al.*, 2002), fluorescence quenching (Harris *et al.*, 2002), and NMR spectroscopy (Luptak *et al.*, 2001; Tanaka *et al.*, 2002), but provided a local view of the regions that undergo structural changes. In conjunction with other metal ion-mediated cleavages of the RNA backbone (e.g., to control for effects given by the different charge on Tb^{3+} compared to Mg^{2+}), in-line probing (Regulski and Breaker, 2008; Soukup and Breaker, 1999), SHAPE (Chapter 4 of this volume), hydroxyl-radical footprinting (Chapters 2 and 3 of this volume), and structural information derived from X-ray crystallography, this approach has the potential to significantly contribute to the understanding of the structural changes associated to binding events or changes in conditions (such as pH, concentration of monovalent cations, etc.).

Finally, UO^{2+} has been proposed as a probe to monitor solvent exposure of the phosphodiester backbone of nucleic acids (Mollegard and Nielsen, 2000). According to this proposal, cleavage by UO^{2+} could be used in conjunction with hydroxyl-radical footprinting, which reports on the solvent exposure of the carbon atoms of the sugar ring, to determine residues with the phosphoryl group and the sugar ring in a different environment. However, little information is present about the fidelity of this cationic probe of RNA structure.

4. Protocols

4.1. General overview

Metal ion-mediated cleavage of RNA is fairly simple in principle. The RNA is radiolabeled, gel purified, subjected to cleavage in the appropriate condition, and the cleavage pattern is detected by running the cleavage reactions on a denaturing gel and detecting the radioactivity by phosphor-imaging. However, these simple experiments can be complicated by several factors.

First, it is essential to work in RNase-free conditions; therefore, it is critical to always run a blank experiment, with no metal ions and Mg^{2+} only added to the RNA, to ensure that cleavage is due to the added metal ions and not to some RNase present in solution. However, remember that, as noted above, also Mg^{2+} can induce some cleavage in the RNA backbone.

Second, appropriate controls to ensure the homogeneity of the radiolabeled RNA should also be performed: at minimum, a T1 digestion and an alkaline hydrolysis ladder should always be run in gel lanes next to those for the reactions.

Third, different phosphodiester bonds are cleaved at different rates, because of both the multitude of mechanisms of nucleic acid cleavage and the idiosyncratic nature of local environments within a complex macromolecule such as RNA. This means that in these experiments there is sometimes no such thing as ''single-hit kinetics.'' In other words, by the time one cleavage event happens, another cleavage event may have happened 10 times, generating fragments that, at least in principle, can be further cleaved. These fragments from secondary cleavage events may be erroneously treated as primary cleavages based on their mobility on the gels. Primary and secondary cleavage events can often be distinguished at least in principle, based on the kinetics of product formation (Fersht, 1999). In practice, many experiments are not performed under ''single-hit kinetics,'' but this is not a problem if the structure of the RNA does not change significantly after the first cleavage event.

Finally, parameters such as temperature, pH, buffer concentration, and reaction time can significantly affect the cleavage pattern. Therefore, it is helpful to perform an initial set of experiments to optimize the conditions, avoiding, for example, extensive degradation of the RNA due to high pH or long reaction times.

4.2. RNA radiolabeling

Radiolabeling is usually performed using ^{32}P. RNA can be radiolabeled at the 5′- or 3′-end. In general, it is advisable to perform both radiolabeling and compare the results, because the cleavage pattern should not be affected by the particular label chosen. Here, we describe simple protocols that are generally applicable to many RNAs, but other techniques (Gimple and Schon, 2005) can also be used.

4.2.1. 5′-Radiolabeling

5′-Radiolabeling is achieved using the bacteriophage T4 polynucleotide kinase (PNK), which transfers the gamma phosphate from γ-^{32}P-ATP to the 5′-hydroxyl terminus of the RNA. RNA obtained from *in vitro* transcription has a 5′-triphosphate, which must be removed prior to 5′-radiolabeling with γ-^{32}P-ATP. Typical yields from a 20 μl reaction are 150 μl of radiolabeled RNA, 300,000 cpm/μl.

4.2.1.1. Removal of the 5′-triphosphate

1. Set up the following reaction:

RNA (~12 μM)	8.0 μl
10× Antarctic phosphatase buffer (500 mM bis-tris-propane–HCl, pH 6.0; 100 mM $MgCl_2$; 10 mM $ZnCl_2$)	1.0 μl
Antarctic phosphatase (5000 units/ml)	1.0 μl
Total volume	10.0 μl

2. Incubate at 37 °C for 30 min.
3. Terminate the reaction by adding 0.8 μl of 250 mM EDTA and incubate at 65 °C for 5 min to denature the phosphatase.
4. Spin down the tubes and proceed to the 5′-radiolabeling reactions.

The quantity of RNA to be radiolabeled may be scaled up or down as needed.

4.2.1.2. Radiolabeling the RNA 5′-end

1. Set up the following reaction:

RNA (from triphosphate removal reaction)	10.8 μl
10× PNK buffer (700 mM Tris–HCl, pH 7.6; 100 mM $MgCl_2$; 50 mM dithiothreitol)	2.0 μl
100 mM $MgCl_2$	1.0 μl
[γ-^{32}P] ATP (160 μCi/μl)	1.0 μl
T4 PNK (10,000 units/ml)	2.0 μl
Water	3.2 μl
Total volume	20.0 μl

2. Incubate at 37 °C for 30 min.
3. (Optional step) Remove unincorporated short fragments by passing the sample through a size-exclusion column such as Bio-Rad P30 microspin column. This step is optional, but will significantly reduce the amount of ''junk'' radioactivity in the sample. Make sure to use a column with a cutoff compatible to the radiolabeled RNA.
4. Add 0.5–1 volumes of loading buffer (8 M urea; 50 mM EDTA, pH 8.0; 0.01% bromophenol blue; 0.01% xylene cyanol) to the resulting solution and proceed to gel purification.

4.2.2. 3′-Radiolabeling

3′-Radiolabeling can be performed using a number of different techniques (Gimple and Schon, 2005). We describe the protocol that uses the Klenow Fragment (3′→5′-exo$^-$) of DNA polymerase I (KF), to incorporate a radiolabeled deoxynucleotide at the 3′-terminus of RNA. The RNA to be labeled is annealed to a short DNA template, which is complementary to

the 3′-end of the RNA and a two-nucleotide overhang at its 5′-end. The Klenow Fragment is then used to extend the 3′-end of RNA by one nucleotide that is complementary to the annealed DNA template. The DNA template should have a dideoxy terminator at its 3′-end to prevent labeling of the primer, leading to decrease in the labeling yield of the RNA. Typical yields from an 80 μl reaction are 100 μl of radiolabeled RNA, 200,000 cpm/μl.

1. Set up the annealing reaction as follows:

10× annealing buffer (140 m*M* Tris–HCl, pH 7.5; 400 m*M* NaCl; 2 m*M* EDTA)	4.0 μl
RNA to be labeled, 10 μ*M*	10.0 μl
DNA template, 30 μ*M*	4.2 μl
Water	25.8 μl
Total volume	40.0 μl

2. Incubate the annealing reaction at 60 °C for 1 min.
3. Cool the reaction for 10 min at room temperature. Spin down the tube.
4. During the 10 min cooling step, prepare the labeling reaction, adding the enzyme last.

20× Klenow Fragment buffer (140 m*M* $MgCl_2$, 20 m*M* DTT)	4.0 μl
Annealing reaction	40.0 μl
[α-^{32}P]-dATP (20 μCi/μl)	8.0 μl
Water	20.0 μl
Klenow Fragment (3′→5′-exo$^-$), 5000 units/ml	8.0 μl
Total volume	80.0 μl

5. Incubate the reaction for 50–60 min at 37 °C. Avoid longer times to reduce the possible incorporation of multiple nucleotides.
6. Concentrate the sample and remove unincorporated short fragments by passing the sample through a size-exclusion column such as Bio-Rad P30 microspin column.
7. Add 0.5–1 volumes of loading buffer (8 *M* urea; 50 m*M* EDTA, pH 8.0; 0.01% bromophenol blue; 0.01% xylene cyanol) to the resulting solution and proceed to gel purification.

4.3. RNA purification

1. Purify the radiolabeled RNA on a denaturing polyacrylamide gel containing 7 *M* urea in TBE buffer (90 m*M* Tris–borate, pH 8.5, 2.5 m*M* EDTA). Run a 0.5 mm thick gel at 50 W using a metal plate for an appropriate amount of time (use bromophenol blue and xylene cyanol as markers).
2. Remove the top plate. Cover with saran wrap.

3. Detect the position of the radioactive bands by exposing a film to the gel in a dark room. Punch holes in the gel using a needle to mark gel and film. Make sure not to poke holes in the radioactive RNA bands.
4. Place the film on a light box and use the punched holes to align the gel.
5. Cut out the gel area corresponding to the desired bands on film. Use sterile scalpels or ethanol-flamed razor blades. Place each band in a different tube.
6. Place the tubes on dry ice and freeze them. Freeze and thaw the gel slices three times.
7. When slices are thawed for the third time, add 150 μl of water or TEN buffer (50 m*M* Tris–HCl, pH 7.5; 10 m*M* EDTA; 0.3 *M* NaCl). Rotate the tubes overnight at 4 °C.
8. Remove traces of acrylamide, concentrate the RNA, and/or exchange the RNA in the appropriate buffer (or water) by using a size-exclusion column such as a Bio-Rad P30 column.
9. (Optional) Perform a phenol/chloroform extraction to remove possible protein contaminants and precipitate the RNA.
10. Dilute the RNA to less than 300,000 cpm/μl to minimize autoradiolysis and store at −20 °C.

4.4. Cleavage reactions

1. Prepare a stock solution of radiolabeled RNA and denature it by heating at 90 °C for 2 min. The amount of radiolabeled RNA should be sufficient for aliquots at each desired metal ion concentration; each reaction should have at least 30,000 cpm/μl.
2. Prefold the RNA by incubating at temperature, salt concentration, and pH optimized for the RNA under investigation.
3. Prepare reaction tubes with aliquots of Mg^{2+} and other components (*except for the cleavage-inducing metal ion*) to obtain the desired final concentrations. Include also a sample with buffer only and one with 10 m*M* EDTA (final concentration).
4. Prepare serial sets of cleaving-inducing metal ion dilutions in water, ranging from micro- to millimolar concentrations. Chloride salts are usually used, except for Pb^{2+}, whose acetate salt is used for cleavage experiments. ($PbCl_2$ is insoluble in water.)
5. Aliquot the prefolded RNA into the tubes previously prepared. Allow 5–10 min to equilibrate. If a potentially reacting substrate is present, ensure that the reaction does not occur in the experiments' time scale.
6. Initiate the metal ion-induced cleavage by adding 2 μl of the proper metal ion solution to the aliquoted RNA in (5).
7. Quench the reaction by adding the appropriate volume of stop solution (90% formamide, 50 m*M* EDTA, pH 8.0, 0.01% bromophenol blue, 0.01% xylene cyanol), so that the concentration of EDTA is at least

twofold the sum of the concentrations of the multivalent metal ions in the reaction aliquot.

8. Separate the cleavage products on a denaturing gel, with the percentage of acrylamide depending on the RNA in study. Use markers, such as RNase T1-digested RNA and alkaline hydrolysis ladder of the RNA in question to identify cleavage sites. In case of long RNAs, use two gels running for different times to resolve different regions of the molecule.
9. Dry the gel under vacuum, 80 °C, for 30–60 min and expose it to a phosphor screen overnight.
10. Align the gel using dedicated software such as SAFA (Das *et al.*, 2005). Quantify the intensity of the cleavage bands using the same program.

4.5. Troubleshooting

- No cleavage detected.
  - The metal ion solution could be too old: prepare a new solution of the metal ion salts.
  - The cleavage conditions are not optimized: vary incubation time, concentration of the metal ions, pH. It may be useful to run a control with single-stranded RNA as standard, to ensure that the conditions used can result in RNA cleavage.
  - The RNA contains a contaminant that interferes with cleavage: try to exchange the RNA in the cleavage buffer or prepare new RNA.
- Complete degradation detected.
  - The concentration of cleaving metal ion is too high: reduce the concentration.
  - The time of incubation is too long: decrease the incubation time.
  - The pH is too high: lower the pH.
  - One or more solutions are contaminated with nucleases. Change all solutions or perform a scan to determine which one(s) is responsible.

ACKNOWLEDGMENT

This research was supported by a grant from the NIH (GM 49243) to D. H.

REFERENCES

Arnone, A., Bier, C. J., Cotton, F. A., Day, V. W., Hazen, E. E. Jr., Richardson, D. C., Yonath, A., and Richardson, J. S. (1971). A high resolution structure of an inhibitor complex of the extracellular nuclease of *Staphylococcus aureus*. I. Experimental procedures and chain tracing. *J. Biol. Chem.* **246,** 2302–2316.

Basu, S., and Strobel, S. A. (1999). Thiophilic metal ion rescue of phosphorothioate interference within the *Tetrahymena* ribozyme P4–P6 domain. *RNA* **5,** 1399–1407.

Brannvall, M., Mikkelsen, N. E., and Kirsebom, L. A. (2001). Monitoring the structure of *Escherichia coli* RNase P RNA in the presence of various divalent metal ions. *Nucleic Acids Res.* **29,** 1426–1432.

Breslow, R., and Huang, D.-L. (1991). Effects of metal ions, including Mg^{2+} and lanthanides, on the cleavage of ribonucleotides and RNA model compounds. *Proc. Natl. Acad. Sci. USA* **88,** 4080–4083.

Brown, R. S., Dewan, J. C., and Klug, A. (1985). Crystallographic and biochemical investigation of the lead(II)-catalyzed hydrolysis of yeast phenylalanine tRNA. *Biochemistry* **24,** 4785–4801.

Butzow, J. J., and Eichhorn, G. L. (1971). Interaction of metal ions with nucleic acids and related compounds. XVII. On the mechanism of degradation of polyribonucleotides and oligoribonucleotides by zinc(II) ions. *Biochemistry* **10,** 2019–2027.

Ciesiolka, J., Wrzesinski, J., Gornicki, P., Podkowinski, J., and Krzyzosiak, W. J. (1989). Analysis of magnesium europium and lead binding sites in methionine initiator and elongator tRNAs by specific metal ion-induced cleavages. *Eur. J. Biochem.* **186,** 71–77.

Ciesiolka, J., Michalowski, D., Wrzesinski, J., Krajewski, J., and Krzyzosiak, W. J. (1998). Pattern of cleavages induced by lead ions in defined RNA secondary structure motifs. *J. Mol. Biol.* **275,** 211–229.

Dallas, A., Vlassov, A. V., and Kazakov, S. A. (2004). Principles of nucleic acid cleavage by metal ions. *In* ''Nucleic Acids and Molecular Biology,'' (M.A Zenkova, ed.), Vol. 13, pp. 61–88. Springer-Verlag, Berlin Heidelberg.

Das, R., Laederach, A., Pearlman, S. M., Herschlag, D., and Altman, R. B. (2005). SAFA: Semi-automated footprinting analysis software for high-throughput identification of nucleic acid footprinting experiments. *RNA* **11,** 344–354.

Dimroth, K., Jaenicke, L., and Heinzel, D. (1950). Die Spaltung Der Pentose-Nucleinsaure Der Hefe Mit Bleihydroxyd. 1. Uber Nucleinsauren. *Annalen Der Chemie-Justus Liebig* **566,** 206–210.

Dorner, S., and Barta, A. (1999). Probing ribosome structure by europium-induced RNA cleavage. *Biol. Chem.* **380,** 243–251.

Farkas, W. R. (1968). Depolymerization of ribonucleic acid by plumbous ion. *Biochim. Biophys. Acta* **155,** 401–409.

Fedor, M. J. (2002). The role of metal ions in RNA catalysis. *Curr. Opin. Struct. Biol.* **12,** 289–295.

Fersht, A. (1999). Structure and Mechanism in Protein Science. W.H. Freeman and Company, New York.

Frederiksen, J. K., Fong, R., and Piccirili, J. A. (2009). Metal ions in RNA catalysis. *In* ''Nucleic Acid-Metal Ion Interactions,'' (N. V. Hud, ed.), Royal Society of Chemistry, Cambridge, UK.

Gimple, O., and Schon, A. (2005). Direct determination of RNA sequence and modification by radiolabeling methods. *In* ''Handbook of RNA Biochemistry,'' (R. K. Hartmann, ed.), Vol. 1, pp. 132–150. Wiley-VCH Verlag GmbH & Co., Weinheim.

Hall, J., Husken, D., and Haner, R. (1996). Towards artificial ribonucleases: The sequence-specific cleavage of RNA in a duplex. *Nucleic Acids Res.* **24,** 3522–3526.

Hargittai, M. R. S., Mangla, A. T., Gorelick, R. J., and Musier-Forsyth, K. (2001). HIV-1 neurocapsid protein zinc finger structures induce tRNALys, 3 structural changes but are not critical for primer/template annealing. *J. Mol. Biol.* **312,** 985–997.

Harris, D. A., Rueda, D., and Walter, N. G. (2002). Local conformational changes in the catalytic core of the trans-acting hepatitis delta virus ribozyme accompany catalysis. *Biochemistry* **41,** 12051–12061.

Huff, J. W., Sastry, K. S., Gordon, M. P., and Wacker, W. E. (1964). The action of metal ions on tobacco mosaic virus ribonucleic acid. *Biochemistry* **3,** 501–506.

Husken, D., Goodall, G., Blommers, M. J., Jahnke, W., Hall, J., Haner, R., and Moser, H. E. (1996). Creating RNA bulges: Cleavage of RNA in RNA/DNA duplexes by metal ion catalysis. *Biochemistry* **35,** 16591–16600.

Jack, A., Ladner, J. E., Rhodes, D., Brown, R. S., and Klug, A. (1977). A crystallographic study of metal-binding to yeast phenylalanine transfer RNA. *J. Mol. Biol.* **111,** 315–328.

Jeong, S., Sefcikova, J., Tinsley, R. A., Rueda, D., and Walter, N. G. (2003). Trans-acting Hepatitis Delta Virus ribozyme, catalytic core and global structure are dependent on the 5′ substrate sequence. *Biochemistry* **42,** 7727–7740.

Kaye, N. M., Zahler, N. H., Christian, E. L., and Harris, M. E. (2002). Conservation of helical structure contributes to functional metal ion interactions in the catalytic domain of ribonuclease P RNA. *J. Mol. Biol.* **324,** 429–442.

Kazakov, S., and Altman, S. (1991). Site-specific cleavage by metal ion cofactors and inhibitors of M1 RNA, the catalytic subunit of RNase P from *Escherichia coli*. *Proc. Natl. Acad. Sci. USA* **88,** 9193–9197.

Kazantsev, A. V., Krivenko, A. A., and Pace, N. R. (2009). Mapping metal-binding sites in the catalytic domain of bacterial RNase P RNA. *RNA* **15,** 266–276.

Kirsebom, L. A., and Ciesiolka, J. (2005). Pb2+-induced cleavage of RNA. *Handb. RNA Biochem.* **1,** 214–228.

Kolasa, K. A., Morrow, J. R., and Sharma, A. P. (1993). Trivalent lanthanide ions do not cleave RNA in DNA–RNA hybrids. *Inorg. Chem.* **32,** 3983–3984.

Krzyzosiak, W. J., Marciniec, T., Wiewiorowski, M., Romby, P., Ebel, J. P., and Giege, R. (1988). Characterization of the lead (II)-induced cleavages in tRNA in solution and effect of the Y-base removal in yeast $tRNA^{Phe}$. *Biochemistry* **27,** 5771–5777.

Lafontaine, D. A., Ananvoranich, S., and Perreault, J.-P. (1999). Presence of a coordinated metal ion in a trans-acting antigenomic *delta* ribozyme. *Nucleic Acids Res.* **27,** 3236–3243.

Luptak, A., Ferre-D'Amare, A. R., Zhou, K. H., Zilm, K. W., and Doudna, J. A. (2001). Direct pK(a) measurement of the active-site cytosine in a genomic hepatitis delta virus ribozyme. *J. Am. Chem. Soc.* **123,** 8447–8452.

Matysiak, M., Wrzesinski, J., and Ciesiolka, J. (1999). Sequential folding of the genomic ribozyme of the Hepatitis Delta Virus: Structural analysis of RNA transcription intermediates. *J. Mol. Biol.* **291,** 283–294.

Mikkola, S., Kaukinen, U., and Lonnberg, H. (2001). The effect of secondary structure on cleavage of the phosphodiester bonds of RNA. *Cell Biochem. Biophys.* **34,** 95–119.

Mollegard, N. E., and Nielsen, P. E. (2000). Application of uranyl cleavage mapping of RNA structure. *Methods Enzymol.* **318,** 43–47.

Oivanen, M., Kuusela, S., and Lonnberg, H. (1998). Kinetics and mechanisms for the cleavage and isomerization of the phosphodiester bonds of RNA by Bronsted acids and bases. *Chem. Rev.* **98,** 961–990.

Pereira, M. J. B., Harris, D. A., Rueda, D., and Walter, N. G. (2002). Reaction pathway of the trans-acting hepatitis delta virus ribozyme: A conformational change accompanies catalysis. *Biochemistry* **41,** 730–740.

Rangan, P., and Woodson, S. A. (2003). Structural requirement for Mg^{2+} binding in the group I intron core. *J. Mol. Biol.* **329,** 229–238.

Regulski, E. E., and Breaker, R. R. (2008). In-line probing analysis of riboswitches. *Methods Mol. Biol.* **419,** 53–67.

Rogers, J., Chang, A. H., Von Ahsen, U., Schroeder, R., and Davies, J. (1996). Inhibition of the self-cleaving reaction of the human Hepatitis Delta Virus ribozyme by antibiotics. *J. Mol. Biol.* **259,** 916–925.

Sampson, J. R., Sullivan, F. X., Behlen, A. B., DiRenzo, O. C., and Uhlenbeck, O. C. (1987). Characterization of two RNA-catalyzed RNA cleavage reactions. *Cold Spring Harbor Symp. Quant. Biol.* **52,** 267–275.

Sigel, R. K. O., Vaidya, A., and Pyle, A. M. (2000). Metal ion binding sites in a group II intron core. *Nat. Struct. Biol.* **7,** 111–116.

Soukup, G. A., and Breaker, R. R. (1999). Relationship between internucleotide linkage geometry and the stability of RNA. *RNA* **5,** 1308–1325.

Stahley, M. R., and Strobel, S. A. (2007). Structural metals in the group I intron: A ribozyme with a multiple metal ion core. *J. Mol. Biol.* **372,** 89–102.

Streicher, B., von Ahsen, U., and Schroeder, R. (1993). Lead cleavage sites in the core structure of group I intron-RNA. *Nucleic Acids Res.* **21,** 311–317.

Streicher, B., Westhof, E., and Schroeder, R. (1996). The environment of two metal ions surrounding the splice site of a group I intron. *EMBO J.* **15,** 2256–2264.

Tanaka, Y., Tagaya, M., Hori, T., Sakamoto, T., Kurihara, Y., Katahira, M., and Uesugi, S. (2002). Cleavage reaction of HDV ribozymes in the presence of Mg^{2+} is accompanied by a conformational change. *Genes Cells* **7,** 567–579.

Travers, K. J., Boyd, N., and Herschlag, D. (2007). Low specificity of metal ion binding in the metal ion core of a folded RNA. *RNA* **13,** 1205–1213.

Westheimer, F. H. (1968). Pseudo-rotation in the hydrolysis of phosphate esters. *Acc. Chem. Res.* **1,** 70–78.

Winter, D., Polaceck, N., Halama, I., Streicher, B., and Barta, A. (1997). Lead-catalysed specific cleavage of ribosomal RNAs. *Nucleic Acids Res.* **25,** 1817–1824.

Zagorowska, I., Kuusela, S., and Lonnberg, H. (1998). Metal ion-dependent hydrolysis of RNA phosphodiester bonds within hairpin loops. A comparative kinetic study on chimeric ribo/2′-*O*-methylribo oligonucleotides. *Nucleic Acids Res.* **26,** 3392–3396.

Zivarts, M., Liu, Y., and Breaker, R. R. (2005). Engineered allosteric ribozymes that respond to specific divalent metal ions. *Nucleic Acids Res.* **33,** 622–631.